Journal of Controlled Release xxx (2016) xxx–xxx

Contents lists available at ScienceDirect

Journal of Controlled Release

journal homepage: www.elsevier.com/locate/jconrel

Hyaluronic acid coated PLGA nanoparticulate docetaxel effectively targets and suppresses orthotopic human lung cancer

Jintian Wu, Chao Deng *, Fenghua Meng, Jian Zhang, Huanli Sun, Zhiyuan Zhong *

Biomedical Polymers Laboratory, College of Chemistry, Chemical Engineering and Materials Science, Soochow University, Suzhou 215123, People's Republic of China

ARTICLE INFO

Article history:
Received 21 December 2016
Accepted 22 December 2016
Available online xxxx

Keywords:
PLGA nanoparticles
Docetaxel
Coating
Nanomedicine
Lung cancer

ABSTRACT

PLGA nanotherapeutics though representing a most promising platform for targeted cancer therapy are confronted with low stability and insufficient tumor cell uptake. Here, we report that hyaluronic acid (HA) coated PLGA nanoparticulate docetaxel (DTX-HPLGA) is particularly robust and can effectively target and suppress orthotopic human lung cancer. DTX-HPLGA was easily prepared with a small size of 154 nm and negative surface charge of −22.7 mV by nanoprecipitation and covalent coating with HA. DTX-HPLGA displayed a low IC_{50} of 0.91 μg/mL in CD44+ A549 cells and a prolonged elimination half-life of 4.13 h in nude mice. Interestingly, DTX-HPLGA demonstrated 4.4-fold higher accumulation in the cancerous lung than free DTX, reaching a remarkable level of 13.7 %ID/g at 8 h post-injection, in orthotopic human A549 lung cancer-bearing mice. Accordingly, DTX-HPLGA exhibited significantly better inhibition of tumor growth than free DTX, leading to healthy mice growth and markedly improved survival time. DTX-HPLGA with easy fabrication, excellent stability and tumor accumulation, effective tumor suppression, and low side effects is of particular interest for targeted chemotherapy of lung cancers.

1. Introduction

With increasing incidence and mortality, lung cancer especially non-small cell lung cancer (NSCLC) has emerged as a leading malignancy worldwide [1]. Docetaxel (DTX), a cell cycle-specific antitumor drug that can inhibit the depolymerization of microtubules, has been approved as first- and second-line treatment for NSCLC [2,3]. The clinical formulation of DTX in polysorbate 80 (Taxotere®), however, causes serious side effects including hypersensitivity reactions, nephrotoxicity, and cardiotoxicity [4,5]. To reduce systemic side effects and further improve therapeutic efficacy, various nanocarriers including polymeric micelles, nanoparticles, and liposomes have been explored for DTX delivery [6–8]. Interestingly, polymeric DTX nanoformulations based on e.g. poly(ethylene glycol)-b-poly(D,L-lactide) (PEG-PDLLA), PEG-b-poly(*N*-(2-hydroxypropyl)-methacrylamide-lactate), or cyclodextrin-PEG are under clinical investigation for treating various advanced solid tumors [9–11].

PLGA nanoparticles with excellent biocompatibility and biodegradability are one of the most attractive pharmaceutical delivery nanoplatforms [12–15]. Protein and peptide nanoformulations based on PLGA are currently used for the treatment of various diseases including cancer [16–18]. BIND-014, an active targeting micellar DTX formulation based on PEG-PLGA copolymer, has been under clinical translation for treating advanced solid tumors and NSCLC [19,20]. It should be noted, however, that current PLGA-based nanotherapeutics typically suffers from a low plasma stability, premature drug release, poor tumor accumulation and retention, and inefficient tumor cell uptake [21–23]. PLGA-based nanotherapeutics are usually fabricated using poly(vinyl alcohol), poloxamer, poly(vinyl pyrrolidone) and TPGS as surfactants [24–26], which gives an "inert" surface hindering target cell internalization. Moreover, these surfactants are prone to washing off during purification or in circulation, resulting in destabilization and aggregation of nanotherapeutics [27,28]. Interestingly, Zhang et al. reported that coating of PLGA nanotherapeutics with the plasma membrane of human platelets exhibited reduced cellular uptake by macrophage-like cells and enhanced therapeutic efficacy in a rat model of coronary restenosis and a mouse model of systemic bacterial infection [29]. Chen et al. demonstrated that PLGA nanoparticles following the lipid coating and AMD3100 decoration could efficiently deliver sorafenib and overcome acquired drug resistance in the orthotopic hepatocellular carcinoma model [30]. García-Salcedo et al. reported that PEG and antibody fragment covalently coated PLGA nanoparticulate pentamidine could cure all infected mice at a 10-fold lower dose than the minimal full curative dose of free drug using a murine model of African trypanosomiasis [31]. We recently reported a facile approach to prepare hyaluronic acid (HA) coated PLGA nanoparticles (HPLGA) using vitamin E-oligo(methyl diglycol L-glutamate) (VEOEG) as a surfactant [32]. Paclitaxel-loaded HPLGA exhibited effective inhibition of subcutaneously implanted MCF-7 breast tumor xenografts.

* Corresponding authors.
E-mail addresses: cdeng@suda.edu.cn (C. Deng), zyzhong@suda.edu.cn (Z. Zhong).

http://dx.doi.org/10.1016/j.jconrel.2016.12.024
0168-3659/

In this paper, we report that HA coated PLGA nanoparticulate docetaxel (DTX-HPLGA) effectively targets and suppresses orthotopic human lung cancer (Scheme 1). It is known that lung cancers like A549 are overexpressing CD44 receptors [33–35]. Several studies have shown that HA based self-assembled nanoparticles can effectively deliver therapeutic nucleic acid, siRNA, and microRNA to both sensitive and resistant A549 lung cancer cells, achieving targeted treatment of solid and metastatic tumors *in vivo* [36,37]. HA coating of lipid/starch-based nanomedicines via electrostatic attraction has shown better antitumor efficacy toward lung cancer cells *in vitro* and *in vivo* [38,39]. DTX-HPLGA, unlike previous reported PLGA nanotherapeutics, is easy to fabricate and possesses multi-functions such as enhanced colloidal stability, superb tumor accumulation, and high specificity toward orthotopic human lung cancer in nude mice.

2. Materials and methods

2.1. Preparation of DTX-HPLGA

DTX-HPLGA was prepared by a modified nanoprecipitation method using VEOEG as a surfactant [40]. Briefly, 30 mg of PLGA and 2.6 mg of DTX were dissolved in acetone (3 mL). 0.9 mL of the resulting solution was dropwise added into VEOEG aqueous solution (0.45 mg/mL, 9 mL) under stirring at room temperature. After evaporating acetone, DTX-PLGA NPs were collected by centrifugation at 12,000 rpm for 10 min and then washed once with deionized water to remove free VEOEG surfactant and free drug. Taking advantages of positively charged amine groups in VEOEG located on the nanoparticles surface, negatively charged HA was facilely coated on the DTX-PLGA NPs via electrostatic interaction followed by covalent conjugation via EDC/NHS coupling method, similar to our previous report for HA coated PTX-PLGA NPs (PTX-HPLGA) [32]. The stability of DTX-PLGA NPs against extensive dilution and in 10% FBS was monitored by DLS measurement ($n = 3$). To monitor the intracellular behaviors and *in vivo* tumor-targetability, near infra-red fluorescence probe Cy5 was grafted on HA [32,41], and then coated on HPLGA to obtain Cy5-labeled HPLGA (Cy5-HPLGA).

The DTX loading level in HPLGA was determined by dissolving DTX-HPLGA in acetonitrile/water (50:50, v/v), filtering through a filter (0.45 μm), and measuring using HPLC. The standard curve was acquired with DTX in acetonitrile/water (50:50, v/v) solutions ranging from 0.05 to 100 μg/mL. Drug loading content (DLC) and drug loading efficiency (DLE) were determined as a previous report [32].

2.2. Pharmacokinetics studies

Pharmacokinetics studies of DTX-HPLGA and free DTX were performed in nude mice (dosage: 5 mg DTX equiv./kg, $n = 3$). The mice were handled under protocols approved by Soochow University Laboratory Animal Center and the Animal Care and Use Committee of Soochow University. At predetermined time points post *i.v.* injection (0.05, 0.25, 0.5, 1, 2, 4, 8, 12 and 24 h for DTX-HPLGA while 2, 5, 10, 30, 60, 120 and 240 min for free DTX), 20 μL of blood was drawn, and briefly sonificated in 1.0 mL of acetonitrile/methanol (v/v = 1:1). After incubating overnight, the blood samples were centrifuged at 13,000 rpm for 20 min to obtain the supernatant. DTX was extracted by evaporating the solvent, and then re-dissolve in 250 μL of acetonitrile for HPLC measurement. The blood circulation followed a typical two compartment model, in which the distribution half-life ($t_{1/2\alpha}$) and elimination half-life ($t_{1/2\beta}$) were calculated according to the following formula: $y = A_1 \times \exp(-x/t_1) + A_2 \times \exp(-x/t_2) + y_0$, wherein $t_{1/2\alpha} = t_1 \times \ln 2$ and $t_{1/2\beta} = t_2 \times \ln 2$. The area under the curve (AUC) was estimated using the formula: $AUC = A_1 \times t_1 + A_2 \times t_2$.

2.3. Ex vivo imaging and biodistribution

Ex vivo imaging of HPLGA was evaluated in orthotopic human A549-Luc lung xenografts that were established by injecting 5×10^6 A549-Luc cells in 50 μL of matrigel/phosphate buffer (PB) mixture (1:4, v:v) into the left lung parenchyma of mice. The tumor size and sites were visualized by the measurement of bioluminescence through IVIS Lumina II imaging system (Caliper Life Sciences, U.S.A.) following the injection of D-luciferin potassium salt solution (15 mg/mL, 100 μL) in PBS. When the tumor luminescence intensity reached about

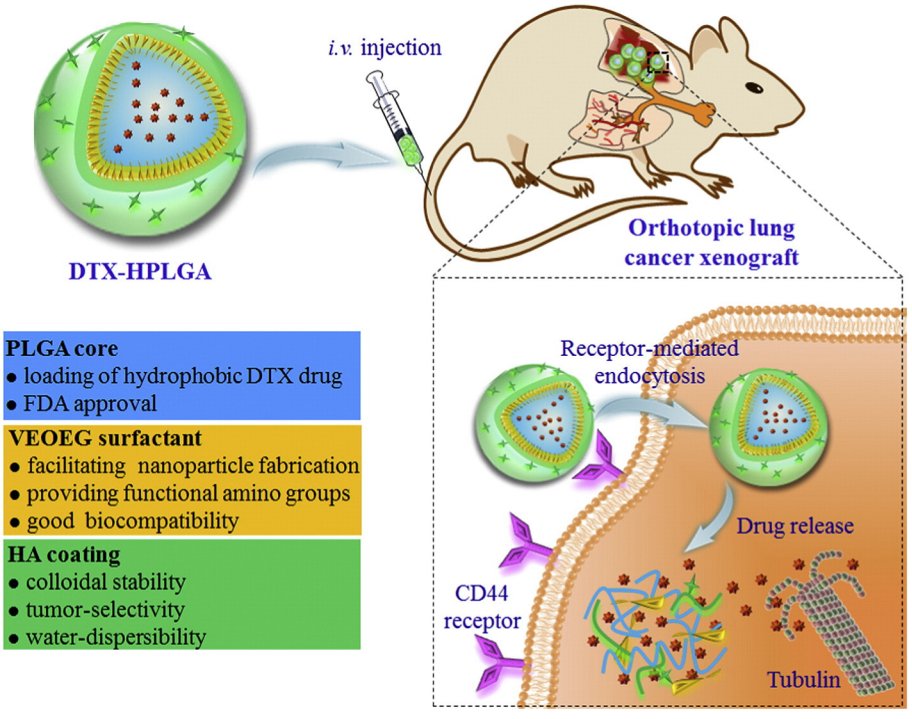

Scheme 1. Illustration of hyaluronic acid (HA) coated PLGA nanoparticulate docetaxel (DTX-HPLGA) that effectively targets and suppresses orthotopic human lung cancer.

Please cite this article as: J. Wu, et al., Hyaluronic acid coated PLGA nanoparticulate docetaxel effectively targets and suppresses orthotopic human lung cancer, J. Control. Release (2016), http://dx.doi.org/10.1016/j.jconrel.2016.12.024

1×10^7 p/s/cm^2/sr, 150 μL of Cy5-HPLGA solution (20 μg/mL) in PBS was intravenously administrated via the tail vein. After 8 h, mice were sacrificed, several major organs (cancerous lung, heart, liver, spleen and kidney) were harvested, and Cy5 fluorescence images were obtained using the IVIS Lumina II imaging system.

To quantify the DTX amount delivered to the tumor and different organs, orthotopic tumor-bearing mice at 8 h post-injection with DTX-HPLGA or free DTX (dosage: 5 mg DTX equiv./kg) were sacrificed, and the cancerous lung and several major organs were harvested, washed, and weighted. DTX was extracted by homogenizing the samples in methanol (2 volumes of tissue) at 20,000 rpm for 1 min, dispersing in 500 μL of acetonitrile, and incubating at −24 °C for 24 h. After 20 min centrifugation at 13,000 rpm, the supernatant was collected, evaporated to dryness, and re-dissolved in acetonitrile (500 μL) for HPLC measurement.

2.4. In vivo antitumor efficacy of DTX-HPLGA

The *in vivo* antitumor efficacy of DTX-HPLGA was assessed using orthotopic human A549-Luc lung cancer xenografts. Treatments were started when luminescence intensity of lung tumor reached about 1×10^6 p/s/cm^2/sr, and this day was designated as day 0. The mice were randomly divided (4 groups, 6 mice/group), and treated with DTX-HPLGA or free DTX (DTX dosage: 5 mg/kg) on day 0, 4, 8 and 12. Bare HPLGA and PBS were used as controls. The treatment effect was assessed by measuring the tumor luminescence intensity. The weight of mice was recorded every other day. Mice were determined to be dead during treatment when the weight loss was over 15%.

2.5. Histological analysis

One mouse of each cohort was sacrificed at day 16 for histological analysis. The lung, liver and kidney were harvested, fixed with paraformaldehyde solution (4%), embedded in paraffin, and cut into 4 μm slices. The slices following the staining with hematoxylin and eosin (H&E) were observed by an optical microscope (Olympus BX41 microscope).

3. Results and discussion

3.1. Preparation and characterization of DTX-HPLGA

DTX-HPLGA was easily prepared through the nanoprecipitation method using VEOEG as a surfactant followed by surface coating with HA via electrostatic interaction and carbodiimide chemistry. The theoretical drug loading content (DLC) was set at 8 wt.%. DLS measurements showed that DTX-HPLGA had a small size with an average diameter of 154 nm and narrow PDI of 0.11 (Fig. 1A). TEM micrograph demonstrated that DTX-HPLGA was spherical and had a size distribution close to that determined by DLS (Fig. 1B). As anticipated, DTX-HPLGA exhibited a negative surface charge of −22.7 mV, in line with coating of nanoparticles with HA [42–44]. HPLC revealed a DLC of 5.5 wt.%, corresponding to a decent drug loading efficiency of 67.5%. Interestingly, DTX-HPLGA displayed a high colloidal stability and could remain a small size and narrow size distribution in serum for over 60 h and at a very low concentration of 1 μg/mL (after 1000-fold dilution) (Fig. S1). Besides, blank HPLGA could maintain their size in PBS at 4 °C for over one month. The long-term storage stability of HPLGA facilitates their clinical use [45–47]. The *in vitro* release studies demonstrated a sustained DTX release from DTX-HPLGA, in which ca. 52.9%, 64.5%, and 73.6% of DTX was released in 7 d at pH 7.4, 5.0, and 4.0, respectively (Fig. 1C). Importantly, no burst drug release was observed, further confirming that DTX-HPLGA has enhanced stability. PLGA NPs often expose a low colloidal stability and/or burst drug release [23,40,48].

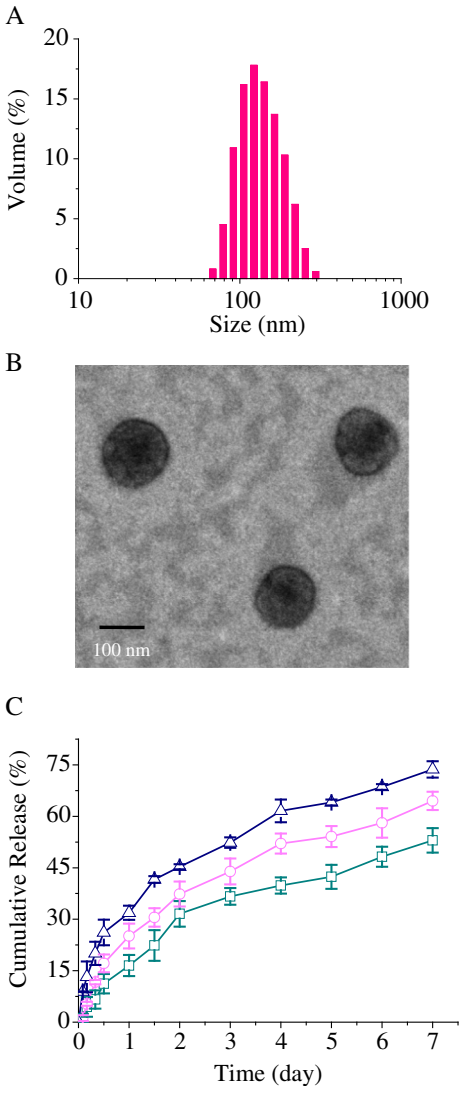

Fig. 1. Size of DTX-HPLGA determined by DLS (A) and TEM (scale bar: 100 nm) (B). (C) *In vitro* drug release profiles of DTX-HPLGA at pH 7.4 (square), 5.0 (circle) and 4.0 (triangle). Data are presented as mean ± SD (n = 3).

3.2. Selectivity and in vitro antitumor activity of DTX-HPLGA

To study their cellular uptake and intracellular delivery path, HPLGA was labeled with Cy5. Flow cytometry revealed that Cy5-HPLGA was efficiently taken up by CD44 receptor-overexpressing A549-Luc cells following 4 h incubation (Fig. 2A). The cellular uptake was, however, significantly reduced by pre-treating A549-Luc cells with free HA. In accordance, confocal microscopy witnessed strong Cy5 fluorescence in the A549-Luc cells following 4 h incubation with Cy5-HPLGA and weak Cy5 fluorescence in free HA-treated A549-Luc cells under otherwise the same conditions (Fig. 2B). These results indicate that HPLGA is taken up by A549-Luc cells via a receptor-mediated mechanism. Therefore, HA coating endows PLGA NPs not only enhanced stability but also better tumor selectivity, which is superior to PLGA NPs decorated with targeting ligands like antibody and peptides [49–51].

Interestingly, our previous results show that bare HPLGA is nontoxic toward normal cells like L929 cells while cause moderate cytotoxicity toward cancerous cells such as MCF-7 and U87MG cells [32]. The selective toxicity of bare HPLGA to cancerous cells originates from vitamin E in the surfactant [52,53]. MTT assays showed a concentration-dependant cytotoxicity of bare HPLGA to A549-Luc cells, where about 60%

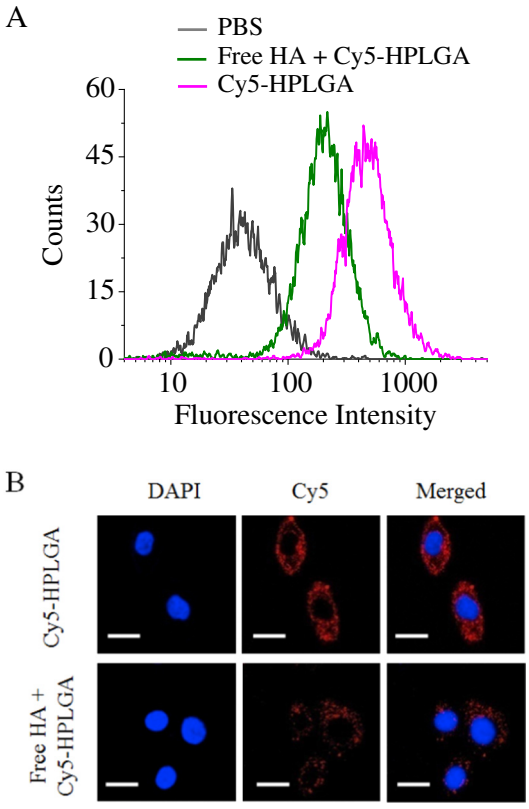

Fig. 2. Flow cytometry and CLSM studies of HPLGA. (A) Flow cytometry of A549-Luc cells following 4 h incubation with Cy5-HPLGA (Cy5 dosage: 5.0 μg/mL). The inhibition experiment was performed by pre-treating cells for 4 h with free HA (5 mg/mL) prior to incubation with Cy5-HPLGA; and (B) CLSM images of A549-Luc cells following 4 h incubation with Cy5-HPLGA (Cy5 dosage: 5.0 μg/mL). For each column, images from left to right show cell nuclei stained by DAPI (blue), Cy5 fluorescence in cells (red) and overlays of above images (scale bar: 20 μm). (For interpretation of the references to colour in this figure legend, the reader is referred to the web version of this article.)

cell viability was discerned at an HPLGA concentration of 600 μg/mL (Fig. 3A). DTX-HPLGA exhibited slightly better antitumor effect to free DTX in A549-Luc cells (IC_{50}: 0.91 *versus* 1.06 μg DTX equiv./mL) (Fig. 3B).

3.3. In vivo pharmacokinetics and biodistribution studies

To study the *in vivo* pharmacokinetics, plasma DTX level at different time intervals following a single *i.v.* injection of 5 mg DTX equiv./kg DTX-HPLGA in nude mice was quantified by HPLC. The results revealed that DTX-HPLGA had a significantly longer circulation time than free DTX (Fig. 4A). The elimination half-lives of DTX-HPLGA and free DTX

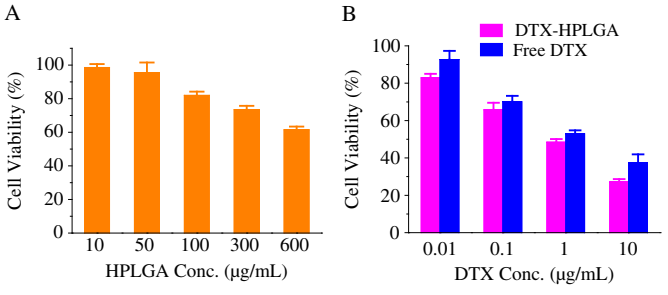

Fig. 3. MTT assays in A549-Luc cells. (A) Bare HPLGA. The cells were incubated with NPs for 48 h; (B) DTX-HPLGA. The cells were treated with DTX-HPLGA for 4 h, the medium was removed and replenished with fresh culture medium, and the cells were incubated for another 44 h. Data are presented as mean ± SD (n = 4).

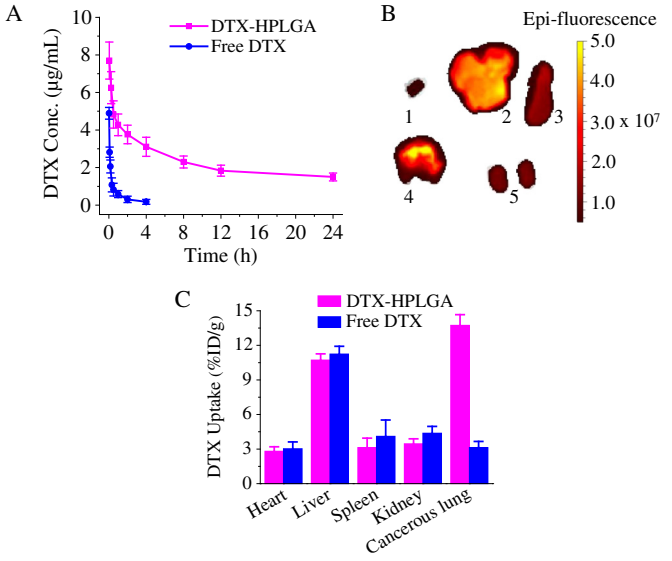

Fig. 4. *In vivo* pharmacokinetics and biodistribution studies. (A) *In vivo* pharmacokinetics of DTX-HPLGA and free DTX in mice (5 mg DTX equiv./kg, n = 3); (B) *ex vivo* Cy5 fluorescence images of the major organs and cancerous lung harvested from the nude mice bearing orthotopic human A549-Luc lung cancer xenografts following 8 h intravenous injection of Cy5-HPLGA (1: Heart, 2: Liver, 3: Spleen, 4: Cancerous lung, and 5: Kidney); and (C) quantification of DTX accumulated in different organs and cancerous lung. DTX uptake is expressed as %ID/g (mean ± SD, n = 3).

were 4.13 h and 0.45 h, respectively (Table S1). In accordance, DTX-HPLGA displayed over 14-fold higher area under the curve (AUC) than free DTX. The long blood circulation time of DTX-HPLGA is likely attributed to their high stability and absence of burst drug release.

Orthotopic human A549-Luc lung xenografts were established by injecting A549-Luc cells with matrigel into the left lung of nude mice [54,55]. The *in vivo* and *ex vivo* imaging showed that strong tumor bioluminescence in the lung following the injection of D-Luciferin potassium salt, indicating successful establishment of orthotopic lung cancers (Fig. S2). To picture the *in vivo* biodistribution of nanovehicles, Cy5-HPLGA was administrated when the tumor luminescence intensity reached about 1×10^7 p/s/cm^2/sr. Interestingly, the *ex vivo* Cy5 fluorescence images displayed strong Cy5 fluorescence in the lung at 8 h post injection, which was far stronger than that in the other major organs like heart, spleen and kidney and close to that in the liver (Fig. 4B), supporting that HPLGA can home to A549-Luc tumor. To accurately determine drug biodistribution, DTX level in different organs of orthotopic A549-Luc tumor-bearing mice following the administration of DTX-HPLGA was quantified using HPLC measurements. Notably, DTX-HPLGA afforded a remarkably high DTX level of 13.7 %ID/g in the lung, which was over 4-fold higher than that with free DTX (Fig. 4C). Moreover, DTX level in the heart, liver, spleen and kidney of mice treated with DTX-HPLGA was slightly lower than or comparable to those with free DTX. These results corroborate that DTX-HPLGA can selectively enhance drug accumulation in the cancerous lung tissue.

3.4. In vivo antitumor efficacy of DTX-HPLGA

It should be noted that in spite of extensive reports on development of nanotherapeutics for lung cancer treatment, most work was based on subcutaneous lung cancer models and only a few studies were performed using orthotopic human lung cancer models [55–59]. The therapeutic efficacy of DTX-HPLGA was evaluated in orthotopic human A549-Luc lung tumor xenografts. The tumor-bearing mice were *i.v.* injected with 5 mg DTX equiv./kg every four days and for a total of four injections. Interestingly, Fig. 5A shows that mice treated with DTX-HPLGA exhibited weak tumor bioluminescence over the whole treatment period of 16 days, corroborating

Please cite this article as: J. Wu, et al., Hyaluronic acid coated PLGA nanoparticulate docetaxel effectively targets and suppresses orthotopic human lung cancer, J. Control. Release (2016), http://dx.doi.org/10.1016/j.jconrel.2016.12.024

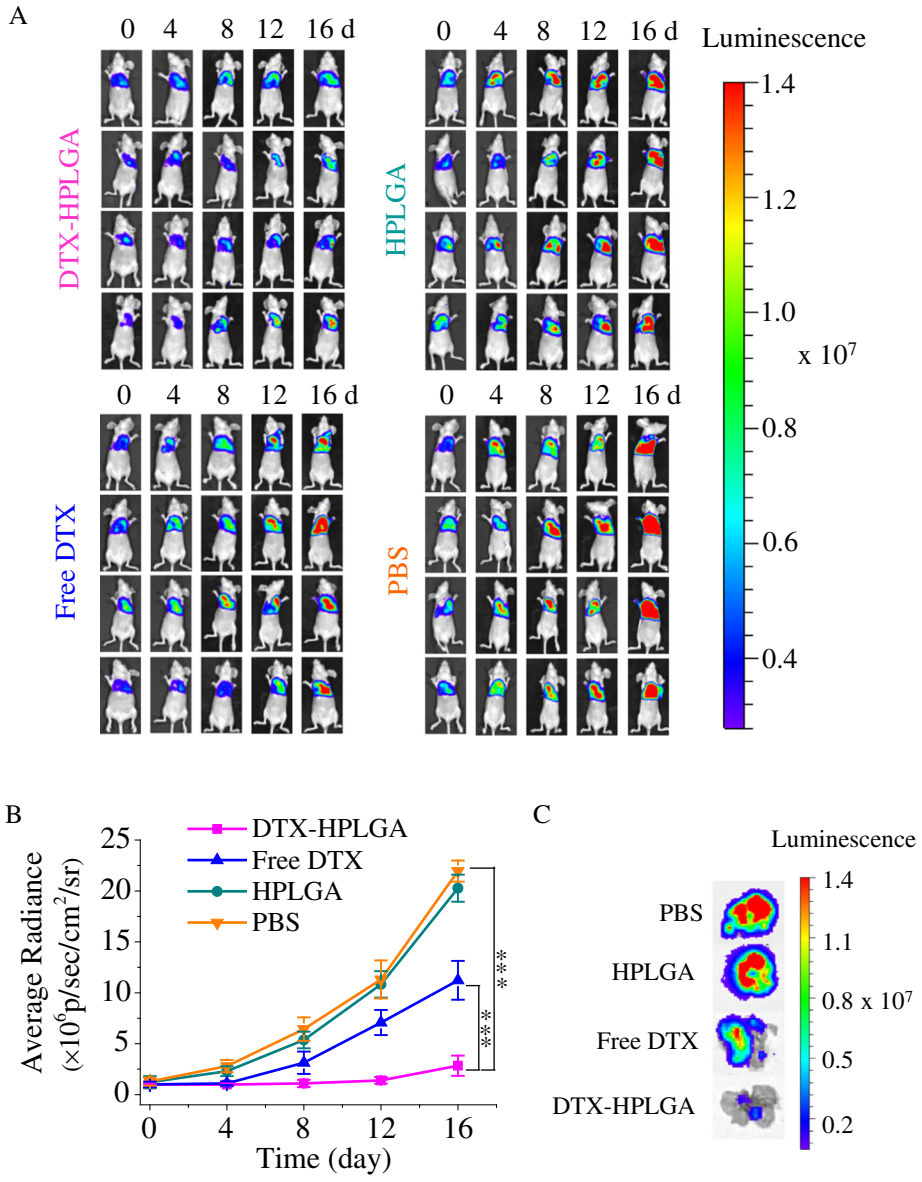

Fig. 5. Tumor volume changes of mice treated with DTX-HPLGA, HPLGA, free DTX, and PBS, respectively. Tumor volume change evaluated by luminescence optical imaging (A) and quantified by average luminescence (B). The *in vivo* luminescent images were normalized and reported as photons per second per centimeter squared per steradian (p/s/cm^2/sr) (mean ± SD, n = 6). ***$p < 0.001$ (Student's *t*-test); and (C) the bioluminescence of cancerous lung on day 16.

that DTX-HPLGA can effectively suppress tumor growth. In comparison, mice treated with free DTX revealed increasing tumor bioluminescence over time, indicating that free DTX exerts less effective tumor inhibition than DTX-HPLGA. Notably, mice treated with bare HPLGA at a comparable nanoparticle concentration to DTX-HPLGA displayed almost the same tumor bioluminescence to those with PBS, insinuating that bare HPLGA at such a low concentration has no antitumor effect *in vivo*. The semi-quantitative analysis of radiance further corroborated that DTX-HPLGA caused significantly more effective tumor inhibition than free DTX (Fig. 5B). The bioluminescence imaging of lung tissues isolated on day 16 confirmed that mice treated with DTX-HPLGA had the weakest tumor luminescence and invasion among all the treatment groups (Fig. 5C). In contrast to control groups treated with PBS or blank HPLGA that possessed numerous white bulges and pleural effusion, as also reported by Mumper et al. for orthotopic human lung cancer xenografts [56], DTX-HPLGA group exhibited relatively smooth and healthy lung surface.

Fig. 6A shows that mice treated with bare HPLGA and PBS exhibited gradual body weight loss in 16 days likely due to lung tumor invasion and malfunction. On the contrary, DTX-HPLGA group continued to grow over time, corroborating effective suppression of tumor invasion and little adverse effects of DTX-HPLGA. Strikingly, DTX-HPLGA significantly improved the survival rates of tumor-bearing mice with all mice survived over an experimental period of 46 days (Fig. 6B). In contrast, mice treated with free DTX, HPLGA and PBS all died in 46 days and had a median survival time of 34, 24 and 20 days, respectively. It is interesting to note that as compared to previously reported liposomal and PLGA nanoparticulate DTX [56–58], DTX-HPLGA appeared more effectively improved the survival rate of orthotopic lung cancer-bearing mice over free DTX, likely as a result of its superior colloidal stability and tumor-

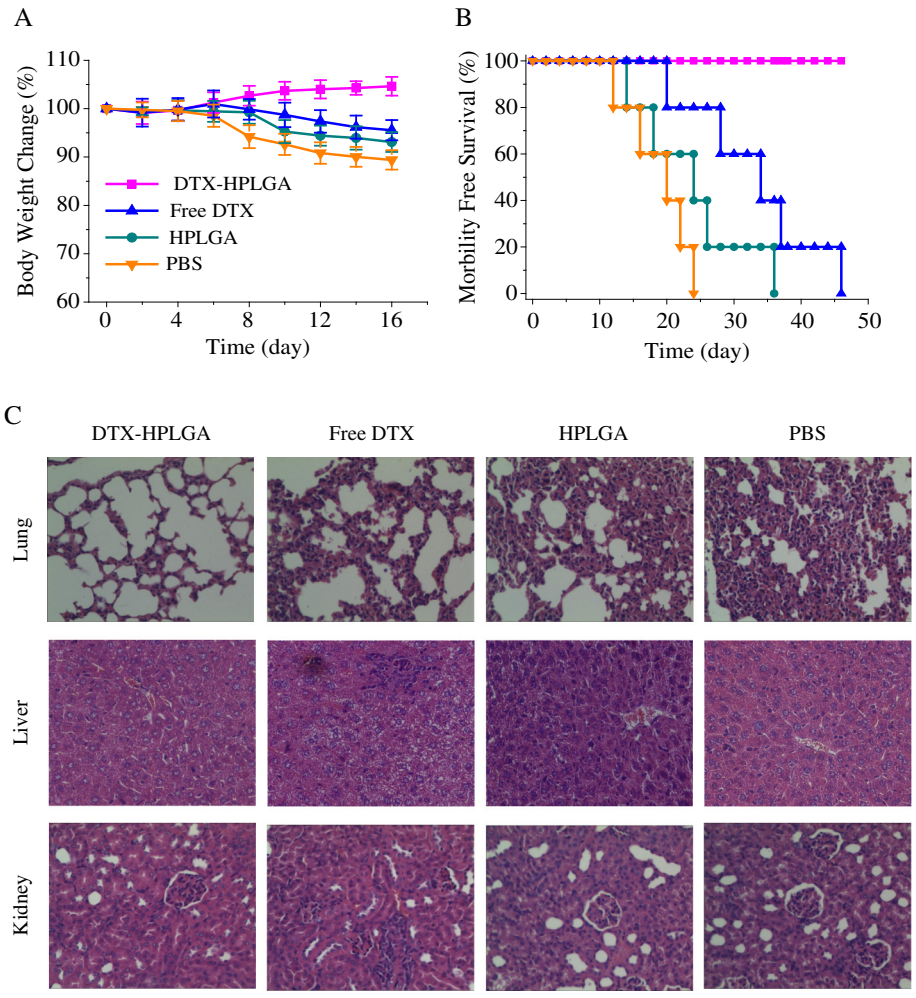

Fig. 6. *In vivo* antitumor performance of DTX-HPLGA in orthotopic human A549-Luc lung tumor-bearing nude mice. (A) Body weight changes of mice treated with DTX-HPLGA, HPLGA, free DTX, or PBS within 16 days (mean ± SD, n = 6); (B) survival rates of mice in different treatment groups within 46 days (mean ± SD, n = 5); (C) histological analysis of the lung, liver, and kidney of mice following 16 days treatment with different formulations. The images were obtained at high magnification (400×).

selectivity. Fig. 6C revealed that bare HPLGA and PBS groups had widespread lung damage with significant disruption of alveolar structure while DTX-HPLGA group maintained well-organized lung tissue. Moreover, in compared to free DTX, DTX-HPLGA induced significantly less damage to the liver and kidney. It is evident that DTX-HPLGA can effectively target and suppress orthotopic human A549-Luc lung cancers, affording significantly improved survival rates and markedly reduced systemic side effects as compared to free DTX.

4. Conclusions

We have demonstrated that hyaluronic acid coated PLGA nanoparticulate docetaxel (DTX-HPLGA) is particularly robust, and can effectively target and suppress orthotopic human A549-Luc lung cancer in nude mice, resulting in greatly improved survival rates and reduced systemic side effects as compared to free DTX. To the best of our knowledge, this represents the first development of multifunctional DTX nanotherapeutics based on PLGA via direct surface coating with hyaluronic acid for targeted lung cancer chemotherapy. Hyaluronic acid coating endows PLGA NPs not only enhanced colloidal stability but also superior tumor cell selectivity *in vitro* and *in vivo*. DTX-HPLGA exhibits prolonged circulation time, a remarkably high accumulation in the cancerous lung (13.7 %ID/g), effective tumor inhibition and low off-target toxicity. It should further be noted that DTX-HPLGA is easy to fabricate, which renders it particularly interesting for further clinical translation.

Acknowledgments

This work was supported by the National Natural Science Foundation of China (NSFC 51273137, 51473110, 51403147, 51225302), and a Project Funded by the Priority Academic Program Development of Jiangsu Higher Education Institutions.

Appendix A. Supplementary data

Supplementary data to this article can be found online at http://dx.doi.org/10.1016/j.jconrel.2016.12.024.

References

[1] L.A. Torre, F. Bray, R.L. Siegel, J. Ferlay, J. Lortet-Tieulent, A. Jemal, Global cancer statistics, 2012, CA Cancer J. Clin. 65 (2015) 87–108.
[2] Y.Z. Min, J.M. Caster, M.J. Eblan, A.Z. Wang, Clinical translation of nanomedicine, Chem. Rev. 115 (2015) 11147–11190.
[3] K. Hotta, Y. Fujiwara, K. Kiura, N. Takigawa, M. Tabata, H. Ueoka, M. Tanimoto, Relationship between response and survival in more than 50,000 patients with advanced non-small cell lung cancer treated with systemic chemotherapy in 143 phase III trials, J. Thorac. Oncol. 2 (2007) 402–407.
[4] J. Baker, J. Ajani, F. Scotte, D. Winther, M. Martin, M.S. Aapro, G. von Minckwitz, Docetaxel-related side effects and their management, Eur. J. Oncol. Nurs. 13 (2009) 49–59.
[5] V.A. de Weger, J.H. Beijnen, J.H. Schellens, Cellular and clinical pharmacology of the taxanes docetaxel and paclitaxel–a review, Anti-Cancer Drugs 25 (2014) 488–494.
[6] Q. Tan, X.J. Liu, X.Y. Fu, Q.L. Li, J.F. Dou, G.X. Zhai, Current development in nanoformulations of docetaxel, Expert Opin. Drug Deliv. 9 (2012) 975–990.

[7] L. Zhang, N. Zhang, How nanotechnology can enhance docetaxel therapy, Int. J. Nanomedicine 8 (2013) 2927–2941.
[8] P.X. Zhao, D. Astruc, Docetaxel nanotechnology in anticancer therapy, ChemMedChem 7 (2012) 952–972.
[9] S. Svenson, Clinical translation of nanomedicines, Curr. Opin. Solid State Mater. Sci. 16 (2012) 287–294.
[10] T.M. Sun, Y.S. Zhang, B. Pang, D.C. Hyun, M.X. Yang, Y.N. Xia, Engineered nanoparticles for drug delivery in cancer therapy, Angew. Chem. Int. Ed. 53 (2014) 12320–12364.
[11] Q. Hu, C.J. Rijcken, E. van Gaal, P. Brundel, H. Kostkova, T. Etrych, B. Weber, M. Barz, F. Kiessling, J. Prakash, G. Storm, W.E. Hennink, T. Lammers, Tailoring the physicochemical properties of core-crosslinked polymeric micelles for pharmaceutical applications, J. Control. Release 244 (2016) 314–325.
[12] A. Kumari, S.K. Yadav, S.C. Yadav, Biodegradable polymeric nanoparticles based drug delivery systems, Colloids Surf. B 75 (2010) 1–18.
[13] F. Danhier, E. Ansorena, J.M. Silva, R. Coco, A. Le Breton, V. Preat, PLGA-based nanoparticles: an overview of biomedical applications, J. Control. Release 161 (2012) 505–522.
[14] S. Fredenberg, M. Wahlgren, M. Reslow, A. Axelsson, The mechanisms of drug release in poly(lactic-co-glycolic acid)-based drug delivery systems-a review, Int. J. Pharm. 415 (2011) 34–52.
[15] G.H. Ma, Microencapsulation of protein drugs for drug delivery: strategy, preparation, and applications, J. Control. Release 193 (2014) 324–340.
[16] R.C. Mundargi, V.R. Babu, V. Rangaswamy, P. Patel, T.M. Aminabhavi, Nano/micro technologies for delivering macromolecular therapeutics using poly(D,L-lactide-co-glycolide) and its derivatives, J. Control. Release 125 (2008) 193–209.
[17] T. Vermonden, R. Censi, W.E. Hennink, Hydrogels for protein delivery, Chem. Rev. 112 (2012) 2853–2888.
[18] S. Tan, T. Sasada, A. Bershteyn, K. Yang, T. Ioji, Z. Zhang, Combinational delivery of lipid-enveloped polymeric nanoparticles carrying different peptides for anti-tumor immunotherapy, Nanomedicine 9 (2014) 635–647.
[19] J. Hrkach, D. Von Hoff, M.M. Ali, E. Andrianova, J. Auer, T. Campbell, D. De Witt, M. Figa, M. Figueiredo, A. Horhota, S. Low, K. McDonnell, E. Peeke, B. Retnarajan, A. Sabnis, E. Schnipper, J.J. Song, Y.H. Song, J. Summa, D. Tompsett, G. Troiano, T.V.G. Hoven, J. Wright, P. LoRusso, P.W. Kantoff, N.H. Bander, C. Sweeney, O.C. Farokhzad, R. Langer, S. Zale, Preclinical development and clinical translation of a PSMA-targeted docetaxel nanoparticle with a differentiated pharmacological profile, Sci. Transl. Med. 4 (2012) 128ra139.
[20] D.D. Von Hoff, M.M. Mita, R.K. Ramanathan, G.J. Weiss, A.C. Mita, P.M. LoRusso, H.A. Burris III, L.L. Hart, S.C. Low, D.M. Parsons, S.E. Zale, J.M. Summa, H. Youssoufian, J.C. Sachdev, Phase I study of PSMA-targeted docetaxel-containing nanoparticle BIND-014 in patients with advanced solid tumors, Clin. Cancer Res. 1-7 (2016).
[21] K. Li, B. Liu, Polymer-encapsulated organic nanoparticles for fluorescence and photoacoustic imaging, Chem. Soc. Rev. 43 (2014) 6570–6597.
[22] J. Pan, S.S. Feng, Targeted delivery of paclitaxel using folate-decorated poly(lactide) - vitamin E TPGS nanoparticles, Biomaterials 29 (2008) 2663–2672.
[23] F. Danhier, N. Lecouturier, B. Vroman, C. Jérôme, J. Marchand-Brynaert, O. Feron, V. Préat, Paclitaxel-loaded PEGylated PLGA-based nanoparticles: in vitro and in vivo evaluation, J. Control. Release 133 (2009) 11–17.
[24] S.K. Sahoo, J. Panyam, S. Prabha, V. Labhasetwar, Residual polyvinyl alcohol associated with poly (D,L-lactide-co-glycolide) nanoparticles affects their physical properties and cellular uptake, J. Control. Release 82 (2002) 105–114.
[25] J.U. Menon, S. Kona, A.S. Wadajkar, F. Desai, A. Vadla, K.T. Nguyen, Effects of surfactants on the properties of PLGA nanoparticles, J. Biomed. Mater. Res. Part A 100A (2012) 1998–2005.
[26] Z.P. Zhang, S.W. Tan, S.S. Feng, Vitamin E TPGS as a molecular biomaterial for drug delivery, Biomaterials 33 (2012) 4889–4906.
[27] Y.I. Chung, J.C. Kim, Y.H. Kim, G. Tae, S.Y. Lee, K. Kim, I.C. Kwon, The effect of surface functionalization of PLGA nanoparticles by heparin- or chitosan-conjugated pluronic on tumor targeting, J. Control. Release 143 (2010) 374–382.
[28] M.J. Santander-Ortega, A.B. Jodar-Reyes, N. Csaba, D. Bastos-Gonzalez, J.L. Ortega-Vinuesa, Colloidal stability of pluronic F68-coated PLGA nanoparticles: a variety of stabilisation mechanisms, J. Colloid Interface Sci. 302 (2006) 522–529.
[29] C.-M.J. Hu, R.H. Fang, K.-C. Wang, B.T. Luk, S. Thamphiwatana, D. Dehaini, N. Phu, P. Angsantikul, C.H. Wen, A.V. Kroll, C. Carpenter, M. Ramesh, V. Qu, S.H. Patel, J. Zhu, W. Shi, F.M. Hofman, T.C. Chen, W. Gao, K. Zhang, S. Chien, L. Zhang, Nanoparticle biointerfacing by platelet membrane cloaking, Nature 526 (2015) 118–121.
[30] D.-Y. Gao, T.-T. Lin, Y.-C. Sung, Y.C. Liu, W.-H. Chiang, C.-C. Chang, J.-Y. Liu, Y. Chen, CXCR4-targeted lipid-coated PLGA nanoparticles deliver sorafenib and overcome acquired drug resistance in liver cancer, Biomaterials 67 (2015) 194–203.
[31] J.L. Arias, J.D. Unciti-Broceta, J. Maceira, T. del Castillo, J. Hernandez-Quero, S. Magez, M. Soriano, J.A. Garcia-Salcedo, Nanobody conjugated PLGA nanoparticles for active targeting of African trypanosomiasis, J. Control. Release 197 (2015) 190–198.
[32] J. Wu, J. Zhang, C. Deng, F. Meng, Z. Zhong, Vitamin E-oligo (methyl diglycol L-glutamate) as a biocompatible and functional surfactant for facile preparation of active tumor-targeting PLGA nanoparticles, Biomacromolecules 17 (2016) 2367–2374.
[33] X. Han, Z. Li, J. Sun, C. Luo, L. Li, Y. Liu, Y. Du, S. Qiu, X. Ai, C. Wu, H. Lian, Z. He, Stealth CD44-targeted hyaluronic acid supramolecular nanoassemblies for doxorubicin delivery: probing the effect of uncovalent PEGylation degree on cellular uptake and blood long circulation, J. Control. Release 197 (2015) 29–40.
[34] V. Jeannot, S. Mazzaferro, J. Lavaud, L. Vanwonterghem, M. Henry, M. Arboléas, J. Vollaire, V. Josserand, J.-L. Coll, S. Lecommandoux, Targeting CD44 receptor-positive lung tumors using polysaccharide-based nanocarriers: influence of nanoparticle size and administration route, Nanomedicine: NBM 12 (2015) 921–932.
[35] A.D. Wojcicki, H. Hillaireau, T.L. Nascimento, S. Arpicco, M. Taverna, S. Ribes, M. Bourge, V. Nicolas, A. Bochot, C. Vauthier, Hyaluronic acid-bearing lipoplexes: Physico-chemical characterization and in vitro targeting of the CD44 receptor, J. Control. Release 162 (2012) 545–552.
[36] S. Ganesh, A.K. Iyer, D.V. Morrissey, M.M. Amiji, Hyaluronic acid based self-assembling nanosystems for CD44 target mediated siRNA delivery to solid tumors, Biomaterials 34 (2013) 3489–3502.
[37] M. Talekar, M. Trivedi, P. Shah, Q.J. Ouyang, A. Oka, S. Gandham, M.M. Amiji, Combination wt-p53 and microRNA-125b transfection in a genetically engineered lung cancer model using dual CD44/EGFR-targeting nanoparticles, Mol. Ther. 24 (2016) 759–769.
[38] X.Y. Yang, Y.X. Li, M. Li, L. Zhang, L.X. Feng, N. Zhang, Hyaluronic acid-coated nanostructured lipid carriers for targeting paclitaxel to cancer, Cancer Lett. 334 (2013) 338–345.
[39] K. Li, H. Liu, W. Gao, M. Chen, Y. Zeng, J.J. Liu, L. Xu, D.C. Wu, Mulberry-like dual-drug complicated nanocarriers assembled with apogossypolone amphiphilic starch micelles and doxorubicin hyaluronic acid nanoparticles for tumor combination and targeted therapy, Biomaterials 39 (2015) 131–144.
[40] X.W. Zeng, W. Tao, L. Mei, L.G. Huang, C.Y. Tan, S.S. Feng, Cholic acid-functionalized nanoparticles of star-shaped PLGA-vitamin E TPGS copolymer for docetaxel delivery to cervical cancer, Biomaterials 34 (2013) 6058–6067.
[41] Y. Zhong, J. Zhang, R. Cheng, C. Deng, F. Meng, F. Xie, Z. Zhong, Reversibly crosslinked hyaluronic acid nanoparticles for active targeting and intelligent delivery of doxorubicin to drug resistant CD44+ human breast tumor xenografts, J. Control. Release 205 (2015) 144–154.
[42] T.F. Martens, K. Remaut, H. Deschout, J.F.J. Engbersen, W.E. Hennink, M.J. van Steenbergen, J. Demeester, S.C. De Smedt, K. Braeckmans, Coating nanocarriers with hyaluronic acid facilitates intravitreal drug delivery for retinal gene therapy, J. Control. Release 202 (2015) 83–92.
[43] H. Wang, P. Agarwal, S.T. Zhao, J.H. Yu, X.B. Lu, X.M. He, A near-infrared laser- activated "nanobomb" for breaking the barriers to microrna delivery, Adv. Mater. 28 (2016) 347–355.
[44] S.P. Wang, J.M. Zhang, Y.T. Wang, M.W. Chen, Hyaluronic acid-coated PEI-PLGA nanoparticles mediated co-delivery of doxorubicin and miR-542-3p for triple negative breast cancer therapy, Nanomedicine: NBM 12 (2016) 411–420.
[45] C. Deng, Y.J. Jiang, R. Cheng, F.H. Meng, Z.Y. Zhong, Biodegradable polymeric micelles for targeted and controlled anticancer drug delivery: promises, progress and prospects, Nano Today 7 (2012) 467–480.
[46] M. Talelli, M. Barz, C.J.F. Rijcken, F. Kiessling, W.E. Hennink, T. Lammers, Core-crosslinked polymeric micelles: principles, preparation, biomedical applications and clinical translation, Nano Today 10 (2015) 93–117.
[47] Y. Suzuki, K. Hyodo, Y. Tanaka, H. Ishihara, siRNA-lipid nanoparticles with long-term storage stability facilitate potent gene-silencing in vivo, J. Control. Release 220 (2015) 44–50.
[48] J.B. Huang, H. Zhang, Y. Yu, Y. Chen, D. Wang, G.Q. Zhang, G.C. Zhou, J.J. Liu, Z.G. Sun, D.X. Sun, Y. Lu, Y.Q. Zhong, Biodegradable self-assembled nanoparticles of poly (D,L-lactide-co-glycolide)/hyaluronic acid block copolymers for target delivery of docetaxel to breast cancer, Biomaterials 35 (2014) 550–566.
[49] N. Karra, T. Nassar, A.N. Ripin, O. Schwob, J. Borlak, S. Benita, Antibody conjugated PLGA nanoparticles for targeted delivery of paclitaxel palmitate: efficacy and biofate in a lung cancer mouse model, Small 9 (2013) 4221–4236.
[50] F. Danhier, B. Vroman, N. Lecouturier, N. Crokart, V. Pourcelle, H. Freichels, C. Jerome, J. Marchand-Brynaert, O. Feron, V. Preat, Targeting of tumor endothelium by RGD-grafted PLGA-nanoparticles loaded with paclitaxel, J. Control. Release 140 (2009) 166–173.
[51] C. Fornaguera, A. Dols-Perez, G. Caldero, M.J. Garcia-Celma, J. Camarasa, C. Solans, PLGA nanoparticles prepared by nano-emulsion templating using low-energy methods as efficient nanocarriers for drug delivery across the blood-brain barrier, J. Control. Release 211 (2015) 134–143.
[52] N. Duhem, F. Danhier, V. Preat, Vitamin E-based nanomedicines for anti-cancer drug delivery, J. Control. Release 182 (2014) 33–44.
[53] H.J. Youk, E. Lee, M.K. Choi, Y.J. Lee, J.H. Chung, S.H. Kim, C.H. Lee, S.J. Lim, Enhanced anticancer efficacy of alpha-tocopheryl succinate by conjugation with polyethylene glycol, J. Control. Release 107 (2005) 43–52.
[54] Y. Zou, F. Meng, C. Deng, Z. Zhong, Robust, tumor-homing and redox-sensitive polymersomal doxorubicin: a superior alternative to doxil and caelyx? J. Control. Release 239 (2016) 149–158.
[55] J. Chen, Y. Zou, C. Deng, F. Meng, J. Zhang, Z. Zhong, Multifunctional click hyaluronic acid nanogels for targeted protein delivery and effective cancer treatment in vivo, Chem. Mater. 28 (2016) 8792–8799.
[56] L. Peng, L. Feng, H. Yuan, S.R. Benhabbour, R.J. Mumper, Development of a novel orthotopic non-small cell lung cancer model and therapeutic benefit of 2′-(2-bromohexadecanoyl)-docetaxel conjugate nanoparticles, Nanomedicine: NBM 10 (2014) 1497–1506.
[57] K.S. Chu, A.N. Schorzman, M.C. Finniss, C.J. Bowerman, L. Peng, J.C. Luft, A.J. Madden, A.Z. Wang, W.C. Zamboni, J.M. DeSimone, Nanoparticle drug loading as a design parameter to improve docetaxel pharmacokinetics and efficacy, Biomaterials 34 (2013) 8424–8429.
[58] K. Patel, R. Doddapaneni, N. Chowdhury, C.H.A. Boakye, G. Behl, M. Singh, Tumor stromal disrupting agent enhances the anticancer efficacy of docetaxel loaded PEGylated liposomes in lung cancer, Nanomedicine 11 (2016) 1377–1392.
[59] X. Ma, X. Huang, Z. Moore, G. Huang, J.A. Kilgore, Y. Wang, S. Hammer, N.S. Williams, D.A. Boothman, J. Gao, Esterase-activatable beta-lapachone prodrug micelles for NQO1-targeted lung cancer therapy, J. Control. Release 200 (2015) 201–211.

Please cite this article as: J. Wu, et al., Hyaluronic acid coated PLGA nanoparticulate docetaxel effectively targets and suppresses orthotopic human lung cancer, J. Control. Release (2016), http://dx.doi.org/10.1016/j.jconrel.2016.12.024